RSC Advances

PAPER

View Article Online
View Journal | View Issue

Cite this: *RSC Adv.*, 2024, **14**, 8684

Study on flame retardancy of EPDM reinforced by ammonium polyphosphate

Yifei Chen,[a] Shengping Yi,[a] Xilong Zhang,*[b] Dunfa Shi,[b] Chao Liu,[b] Puwen Rao[b] and Chi Huang *[a]

Currently, the most widely used material for solid rocket motor (SRM) insulation is ethylene propylene diene monomer (EPDM) filled with flame-retardant and ablation-resistant fillers. Researchers have been working hard to find a flame-retardant filler that can simultaneously meet the complex requirements of mechanical strength, density, flame retardancy and ablative performance of the insulation layer. This requires research on the flame retardant properties of flame retardants in oxygen-poor environments. In this paper, ammonium polyphosphate (APP) is used as a flame retardant filler, which is filled into an EPDM premix (p-EPDM) containing fumed silica and aluminum hydroxide to prepare composite materials. By creating an anoxic environment, the flame retardant behavior of APP under anoxic conditions on EPDM was studied. The results show that composites prepared with APP show better flame retardant properties in tests such as limiting oxygen index and UL-94, with less impact on mechanical strength and density. The surface morphology and elemental composition of the composite combustion residues were studied using Raman spectroscopy, scanning electron microscopy (SEM) and energy dispersion spectroscopy (EDS). In an oxygen-depleted environment, APP will thermally decompose to form ammonia, water vapor and phosphorus-containing acidic substances. These gases dilute the flammable gas and reduce the thermal conductivity. The acidic substances containing phosphorus are concentrated on the surface of the pyrolysis layer to promote the formation of the carbon layer. This provides guidance for us to design insulation layer materials with properties that are more in line with actual use requirements.

Received 29th January 2024
Accepted 29th February 2024

DOI: 10.1039/d4ra00733f

rsc.li/rsc-advances

1 Introduction

During the operation of the solid rocket motor (SRM), the combustion chamber is in a high-temperature and high-pressure environment.[1] Therefore, a thermal insulation layer is needed to protect the rocket casing. Ethylene propylene diene monomer (EPDM) rubber has become a widely used base rubber for thermal insulation layers due to its low density.[2,3] By adding functional fillers such as reinforcing fillers, flame retardant fillers, and anti-ablation fillers, the various properties of EPDM composite materials can be improved to meet the actual needs of the insulation layer.[4–7] The various functional fillers currently used have outstanding advantages as well as some disadvantages in terms of single performance. Researchers are constantly focused on how to rationally adjust the addition amount of each filler component so that the composite material can simultaneously meet the complex performance requirements of the insulation layer such as mechanical strength, high flame retardancy, high ablation resistance, and low density. To better optimize existing compositions, it is necessary to study the various behaviors of materials in the combustion chamber.

The high flame retardancy of composite materials can ensure that the heat insulation layer effectively protects the rocket casing during operation. In addition, the process of flame retardant behavior is often accompanied by carbon formation. The level of flame retardant performance also affects the morphology of the carbon layer formed, thereby affecting the ablation resistance of the material. Adding antimony trioxide and halogen flame retardants such as decabromodiphenyl ether or decabromodiphenoxy complex can increase the limiting oxygen index (LOI) value of EPDM rubber.[8,9] However, the development of halogenated flame retardants is limited due to their toxicity and bioaccumulation properties. Metal hydroxide flame retardants such as aluminum hydroxide and magnesium hydroxide have the characteristics of high decomposition temperature and low smoke/toxic gas generation rate. However, metal hydroxides have high polarity and poor compatibility with polymers, easily leading to secondary agglomeration in EPDM matrix. This can create gaps with the polymer interface, thereby reducing the mechanical properties of the material, which can lead to structural damage under the impact of high-temperature gas.[10] In recent years,

[a]College of Chemistry and Molecular Sciences, Wuhan University, Wuhan, 430072, China. E-mail: chihuang@whu.edu.cn
[b]Hubei Sanjiang Aerospace Jianghe Chemical Technology Co., Ltd, Yichang, 444299, China. E-mail: zhangxilong@hnu.edu.cn

researchers have improved the dispersion of metal hydroxides in rubber matrices to a certain extent through nanotechnology and modified dispersion methods.[11,12] Nevertheless, the density of the prepared composite material is high and cannot meet the requirements of low density insulation layer.[13,14]

Ammonium polyphosphate (APP) is a long-chain polyphosphate that was first synthesized from the reaction of phosphorus and ammonia in 1857 and used as a forest fire extinguishing agent. Due to its good flame retardant ability, it is widely used in flame retardant treatments such as coatings, plastics, fabrics, and wood.[15,16] Compared with halogen flame retardants, APP has the advantages of low cost and low toxicity. Researchers have used APP to replace metal hydroxide flame-retardant fillers in epoxy resin to prepare flame-retardant composite materials, which reduced the density of the composite materials and achieved better flame-retardant effects.[17] Addition of APP to rubber materials such as natural rubber has also achieved good improvement in flame retardant properties.[18] Currently, researchers have conducted extensive studies on the flame retardant behavior of APP in EPDM. However, most of the research on the flame retardant mechanism of APP in EPDM was conducted in an oxygen-rich environment, and there are few related studies under oxygen-poor conditions. However, the working environment of SRM is almost always an oxygen-poor environment. Therefore, studying the flame retardant mechanism of APP in EPDM under oxygen-depleted conditions is of great significance for preparing composite materials that meet the performance requirements of SRM insulation layers in actual operation.

In this study, the effect of APP content on the flame retardant properties of EPDM composites was explored. The flame retardant properties of the composite materials were tested through limiting oxygen index (LOI), vertical flammability index and thermogravimetric analysis (TGA). Through scanning electron microscopy (SEM), energy dispersive analysis (EDS), and analysis of condensed phase and related gas phase products, the possible flame retardant mechanism of APP in APP/EPDM composite materials under oxygen-poor environment was explored.

2 Experimental sections

2.1 Materials

EPDM rubber and EPDM precast rubber (p-EPDM) is provided by Hubei Sanjiang Aerospace Jianghe Chemical Technology Co., Ltd. The main component of p-EPDM is EPDM rubber, which the filler includes 15.4 wt% reinforcing filler fumed silica, 7.7 wt% flame retardant filler aluminum hydroxide and a small amount of functional additives. Ammonium polyphosphate (APP, $n > 1000$) was purchased from Shandong Haoshun Chemical Co., Ltd. The vulcanizing agent 2,5-dimethyl-2,5-di(*tert*-butylperoxy) hexane (AD) and the vulcanizing aid dibenzothiazole disulfide (DM) were provided by Sinopharm Chemical Reagent Co., Ltd.

2.2 Preparation of flame-retardant EPDM

The EPDM prefabricated rubber and flame retardant were dried in an oven at 60 °C for 12 hours before use. According to the designed formula (Table 1), EPDM and APP were mixed in an internal mixer at 100 °C for 120 min to form a mixed rubber. The mixed rubber, vulcanizing agent and vulcanizing aid were run several times in an open mill at 80 °C to form a crude rubber and then stored for 8 h before use. The crude rubber was filled into the molds required for different experiments, and then vulcanized in a flat vulcanizer for 120 min at a temperature of 150 °C and a pressure of 120 kg cm^{-2} to obtain APP/EPDM composite samples.

Table 1 Formulations of flame-retardant samples

	Composites (%)				
Sample	EPDM	p-EPDM	APP	AD	DM
EPDM	94.8	—	—	2.4	2.8
EPDM-APP	79.8		15.9	1.9	2.4
EPDM-1	—	94.8	—	2.4	2.8
EPDM-2	—	90.5	4.5	2.3	2.7
EPDM-3	—	86.6	8.6	2.2	2.6
EPDM-4	—	83.0	12.4	2.1	2.5
EPDM-5	—	79.7	15.9	2.0	2.4

2.3 Mechanical property test

Mechanical properties of composite were tested on the CRS-UTM50CA electronic universal material testing machine made by Suzhou Yanuo Tianxia Instrument Co., Ltd with a tensile rate of 200 mm min^{-1} based on Chinese national standard GB/T 528-2009 standard. The hardness test of the composite material was tested using a Shore A durometer in accordance with the GB/T 531.1-2008 standard. The density of the composite is tested by SJ-600GY density tester of Shanghai Shuju Instrument Technology Co., Ltd. The vulcanization performance of the composite material was tested using the BLH-III vulcanization apparatus of Yangzhou Tianfa Testing Machinery Co., Ltd.

2.4 Thermal analysis test

The TGA test was performed on the STA 2500 synchronous thermal analyzer produced by the German NETZSCH company, with a heating rate of 20 °C min^{-1}, a nitrogen flow of 20 mL min^{-1}, and an appropriate sampling amount of 10 mg. Thermogravimetric infrared spectroscopy (TG-IR) tests were performed to 5 mg samples under nitrogen atmosphere with a nitrogen flow of 20 mL min^{-1}. The infrared testing instrument is the Fourier transform infrared spectrometer Nicolet iS-50 provided by Thermo Fisher Scientific Inc. Test temperature was set between 30 °C to 830 °C with a heating rate of 20 °C min^{-1}. TG-IR detection technology was used to identify gas phase products generated during thermal pyrolysis of APP/EPDM composites.

2.5 Flame retardant performance test

LOI used HC-produced by Nanjing Jiangjing Analytical Instrument Company. Type 2 oxygen index meter measurement. According to the ASTM D2863-97 standard, the sample size is set to 100 × 6.7 × 3 mm^3. The UL-94 vertical combustion tests

were operated on CZF-4 horizontal and vertical combustion tester from Nanjing Jiangjing Analytical Instrument Corporation. According to ASTM D3801 standard, the sample size was 127 × 127 × 3 mm and experimental test was repeated five times. The ablation resistance of the samples was tested on an oxygen acetylene ablator (OTA) under 5 s ablation. The linear ablation rate (LAR) was defined as the rate of the height change before and after ablation time.

2.6 Morphological and elemental analysis

SEM images and EDS images of the flame retardant powder and carbon layer were obtained using a Zeiss Merlin Compact scanning electron microscope manufactured by Oxford Instruments, UK. The degree of graphitization and chemical structure of carbon residues were analyzed using Raman components. Before testing, the samples were spray-coated with a gold (platinum) conductive layer.

2.7 Water absorption property test

Water absorption properties of the composites were tested according to Chinese national standard GB/T 1034-2008 standard. The drying oven temperature was set at 75 °C, and the deionized water temperature was constant at 23 °C. Five samples were tested for each group to obtain the average.

3 Results and discussion

3.1 Mechanical properties

The effects of APP content on the mechanical properties, density, water absorption properties and vulcanization properties of EPDM composites are shown in Fig. 1, Tables 2 and 3. As seen from Fig. 1, with the increase in APP content, the tensile strength of EPDM composites decreases slightly, and the elongation at break and hardness gradually increase. When the APP content reaches 15.9 wt%, the tensile strength of the composite material only decreases by 2.2%, while the elongation at break increases by approximately 6.8%. As seen from the vulcanization test results in Table 3, the addition of APP has little effect on the minimum torque M_L, while the $M_H - M_L$ difference between the maximum torque M_H and the minimum torque M_L has a slight increase. This indicates that APP is uniformly dispersed in EPDM under the strong shear provided by the internal mixer. Due to the large polarity difference between

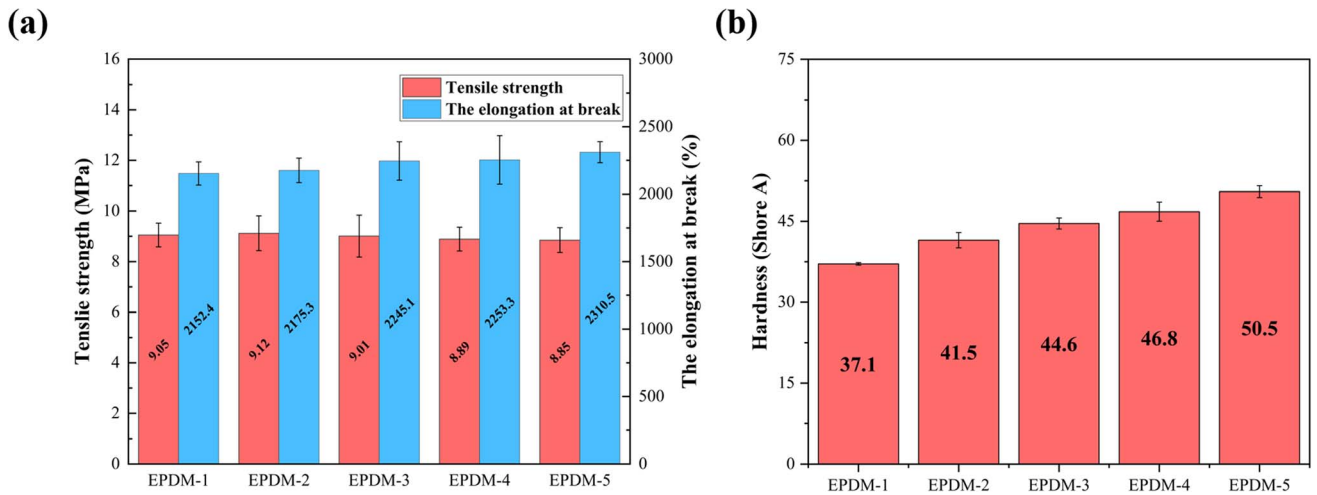

Fig. 1 (a) Stress–strain results and (b) hardness for EPDM and its composites.

Table 2 Mechanical properties of EPDM and its composites

Sample	Tensile strength (MPa)	The elongation at break (%)	Hardness (Shore A)	Density (g cm^{-3})	Water absorption (%)
EPDM	2.86	0.487 × 10^3	34.5	0.890	0.104
EPDM-1	9.85	2.15 × 10^3	37.1	0.989	0.117
EPDM-2	9.12	2.18 × 10^3	41.5	1.013	0.124
EPDM-3	9.01	2.24 × 10^3	44.6	1.027	0.153
EPDM-4	8.89	2.25 × 10^3	46.8	1.042	0.168
EPDM-5	8.85	2.31 × 10^3	50.5	1.063	0.164

Table 3 Vulcanization properties of EPDM and its composite materials

Sample	M_L (N m)	M_H (N m)	$M_H - M_L$ (N m)	t_{90} (s)
EPDM	0.04	0.23	0.19	2084
EPDM-1	0.04	0.25	0.21	2136
EPDM-2	0.04	0.34	0.30	1916
EPDM-3	0.04	0.37	0.33	1846
EPDM-4	0.06	0.44	0.38	1770
EPDM-5	0.07	0.52	0.45	1742

EPDM and APP, a large van der Waals force is induced between them, which allows the adsorption of APP and rubber molecular chains. In the early stages of the rubber stretching process, filler particles can effectively alleviate the phenomenon of stress concentration. The short rubber chains slide on the surface of the rubber particles to allow more chain segments to participate in stress bearing, thereby enhancing the tensile strength of the material. As the elongation further increases, the rubber segments slide through the filler particles, forming a high degree of orientation, allowing the material to withstand greater stresses. During the sliding process of the rubber chain segment, part of the external work is converted into heat by overcoming the sliding friction, further enhancing the mechanical properties of the rubber. Therefore, the filler has a certain reinforcing effect on the rubber. However, the particle size of APP is relatively large, and its incorporation into rubber can cause defects in the rubber. This can easily cause or expand cracks under the action of force, thus reducing the mechanical properties of the material. Under the combined influence of the two, the tensile strength of the material is slightly reduced and the elongation at break is slightly increased. The density test results in Table 2 show that the composite material prepared by APP/EPDM has a lower density, which is conducive to the low-density performance requirements of the insulation layer. The test results of the water absorption properties of APP/EPDM composites are also shown in Table 2. Although the addition of APP improves the water absorption performance of the material, the overall water absorption performance remains at a low level. This is mainly because EPDM itself is a non-polar material and has a certain resistance to polar solutions. On the other hand, the solubility of APP in water decreases with the increasing degree of polymerization. APP with a high degree of polymerization has little solubility in water. In addition, there is a strong van der Waals force between EPDM rubber molecules and APP with high degree of polymerization, which reduces the possibility of APP migration in EPDM. This indicates that the APP/EPDM composite has good water resistance and can still maintain the dispersibility of APP in the composite in a humid environment.

3.2 Simulated combustion test

Simulated combustion test is commonly used to preliminarily evaluate the flame retardant performance of composites, and further analyze the advantages and disadvantages of additives in combination with the relevant test results such as LOI and linear ablation rate, so as to reasonably design composites. The reaction of the samples under small flame was investigated by LOI, UL-94 vertical combustion test and OTA experiment, and the results are shown in Table 4. LOI is often used to evaluate the static flame retardant performance of flame retardant materials. The LOI value of the material exceeds 21%, indicating that it is flame retardant. The higher the LOI value, the better the flame retardancy. The LOI indicates how easily a substance burns. The higher the value, the more difficult it is to burn. LOI of over 27% means that the material is flame retardant. UL-94 is a standard for evaluating the flame retardant properties of rubber. The flame retardancy of rubber is classified according to the phenomenon during the vertical burning test of rubber materials. The influence of flame retardant content on the flame retardant properties of composite materials shows that when the APP content reaches 20%, the flame retardant properties become better. EPDM-5 composite materials can pass UL-94 vertical flame retardant V-0 level test (the flame extinguishes within 10 seconds, allowing dripping of non-burning particles) the LOI and LAR of EPDM-5 composite are 28.1% and 0.151 mm s^{-1} respectively. EPDM raw rubber and EPDM-1 samples without APP have poor flame retardant properties and can only reach the HB level of vertical flame retardancy (the sample burns slowly after ignition, and the burning speed is less than 75 mm min^{-1} for thickness less than 3 mm). Their LOI values are only 16.8% and 19.0%. The above results show that the addition of APP can improve the flame retardant properties of EPDM composite materials.

Table 4 Flammability results of EPDM and its composites[a]

	UL-94			
Sample	Dripping	Rating	LOI (%)	LAR (mm s^{-1})
EPDM	Y	HB	16.8 ± 0.1	0.587 ± 0.001
EPDM-1	Y	HB	19.0 ± 0.2	0.225 ± 0.001
EPDM-2	Y	V-2	22.1 ± 0.2	0.212 ± 0.001
EPDM-3	Y	V-1	24.3 ± 0.3	0.204 ± 0.001
EPDM-4	Y	V-1	27.5 ± 0.2	0.177 ± 0.001
EPDM-5	N	V-0	28.1 ± 0.1	0.151 ± 0.001

[a] N: no; Y: yes.

The morphology of the sample tested by OTA is shown in Fig. 2, and the test results of linear ablation rate are shown in Table 4. The morphological observation shows that with the increase in APP content, the surface morphology of the material gradually becomes complete. An obvious and complete carbon layer structure appears on the surface of EPDM. This implies that the addition of APP promotes carbon formation in composite materials. As the APP content increases, the linear ablation rate of the EPDM composite material decreases significantly, reflecting that APP can improve the ablation performance of the composite material. APP promotes the formation of a carbon layer during the ablation process and plays a protective role in the interior of the composite material.

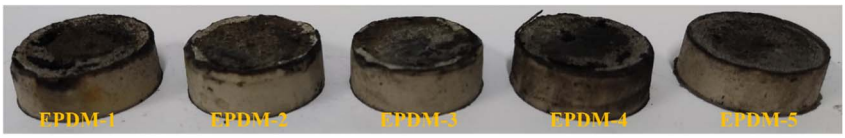

Fig. 2 Photo of EPDM composite after OTA examination.

Since the carbon layer is not easily combustible, the promotion of carbon layer formation by APP can improve the flame retardant performance of the material to a certain extent.

3.3 Thermal stability and gas phase product analysis

Gaseous products from thermal decomposition of APP were analyzed using TG-IR. The TGA and DTG curves of APP are shown in Fig. 3a. The APP sample mainly exhibits three stages of mass loss.[19,20] The first stage appears from 240 °C to 370 °C with a mass loss of 18%, corresponding to the decomposition of APP by heat to generate ammonia. The second stage is from 480 °C to 620 °C with a mass loss rate of about 50%. In this stage, APP is further decomposed to generate metaphosphoric acid and other substances. The third stage of mass loss occurs from 720 °C to 820 °C, and the mass loss rate is 15%, which may be from the evaporation loss of phosphorus-containing components. The TG-IR results of Fig. 3b show that the characteristic absorption peaks of ammonia gas appear at 3400 cm^{-1}, 1630 cm^{-1} and 950 cm^{-1}. In addition, the absorption peak of water vapor appears, indicating that APP produces NH_3 and H_2O in the first stage of mass loss. The thermal decomposition results of APP are consistent with the results reported in the literature, indicating that APP has excellent thermal stability and heat resistance.[20]

Thermal decomposition behavior of APP/EPDM composites under nitrogen atmosphere was investigated by TG test. TGA and DTG curves of EPDM vulcanizates incorporated with different contents of APP in the temperature range from 30 to 830 °C are shown in Fig. 4. $T_{initial}$ is defined as the temperature at which the sample loses 5% of its weight, and T_{max} is defined as the temperature at which the maximum mass loss rate (MLR_{max}) occurs. The experimental data of $T_{initial}$, T_{max}, MLR_{max} and carbon residue rate at 830 °C are shown in Table 5.

TGA curves of composite materials with different APP contents are presented in Fig. 4a. Combined with the decomposition behavior of APP, it is found that the composite material undergoes three stages of mass loss under nitrogen atmosphere. In the first stage at 250–450 °C, the material quality slowly decreases, reflecting the slow process of endothermic dehydration of aluminum hydroxide and thermal decomposition of APP. The second stage is 450–480 °C. During this stage, EPDM rubber begins to decompose, and the rubber main chain begins to break, forming various gas small molecules. The third stage is the second stage of APP decomposition at 480–600 °C to generate metaphosphoric acid and other substances. It is worth noting that the third section of the weight loss process in the APP thermal decomposition curve is not reflected in the thermal decomposition curve of the composite material. This indicates that the decomposition products of the third stage of APP have not detached. The DTG curve in Fig. 4b shows that the peak intensity of EPDM-1 to EPDM-5 samples gradually weakens around 480 °C. The corresponding data in Table 5 show that the MLR_{max} of the material gradually decreases. The possible reason is that the pyrolysis products of APP reduce the diffusion rate of the pyrolysis products of EPDM. As seen from Table 5, with the increase in amount of APP added, $T_{initial}$ gradually decreases, while T_{max} increases slowly. This is likely due to the decomposition behavior of APP caused by heat. APP undergoes the first

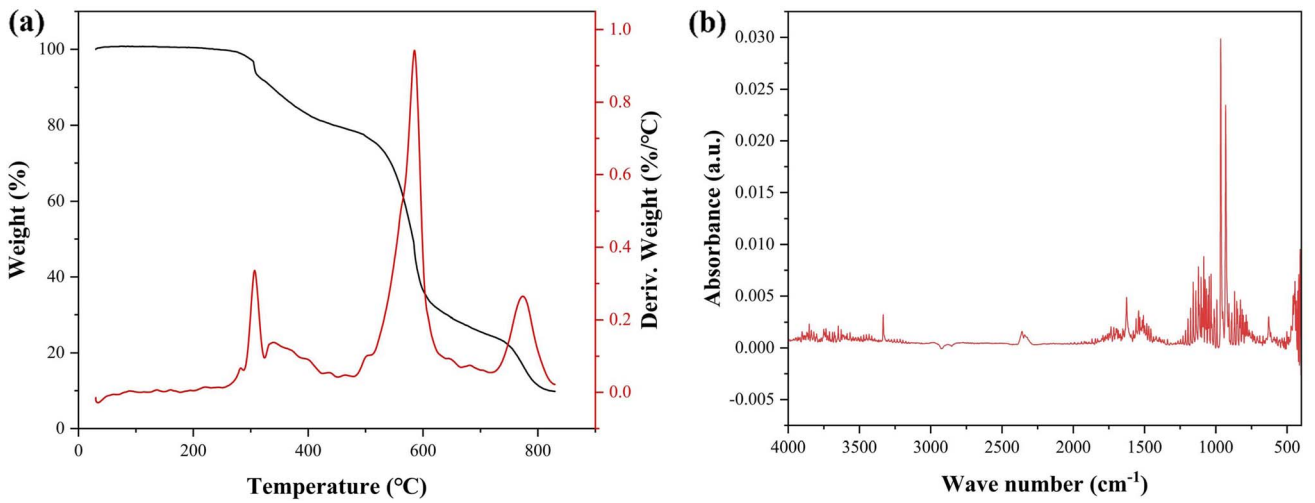

Fig. 3 (a) TGA and DTG curves of APP; (b) infrared curve of APP decomposition gas at 300 °C.

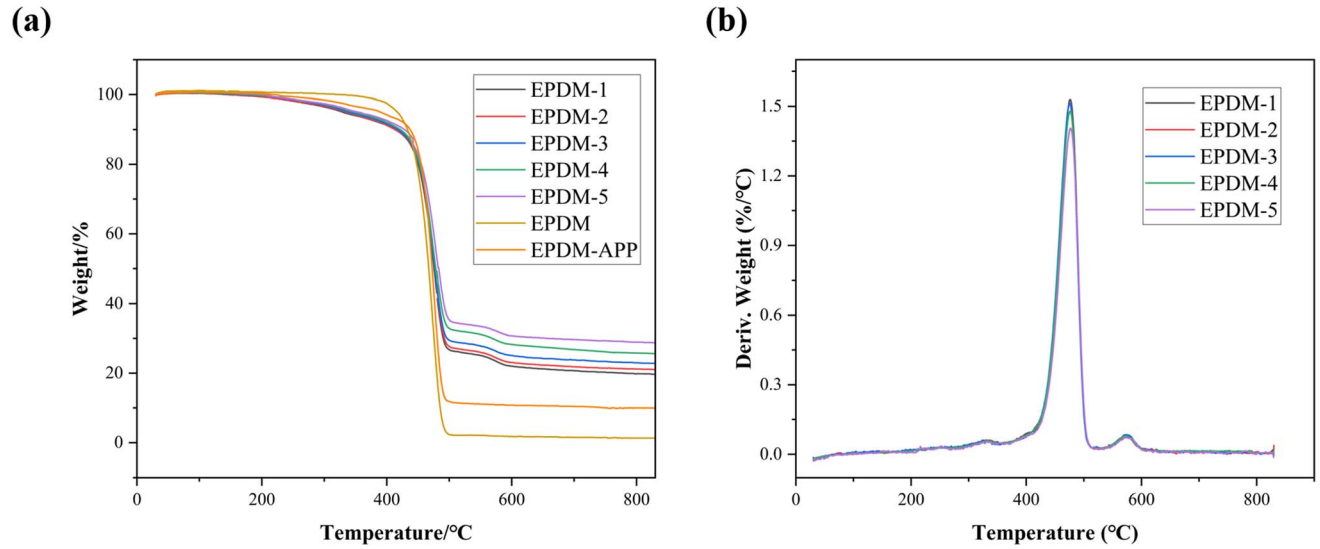

Fig. 4 (a) TGA and (b) DTG curves of APP/EPDM composites.

Table 5 TGA data of APP/EPDM composites

Sample	$T_{initial}$ (°C)	T_{max} (°C)	MLR_{max} (wt% °C^{-1})	Char residue (wt%)	Calculate residue (wt%)
EPDM	—	—	—	1.30	—
EPDM-APP	—	—	—	9.98	2.63
EPDM-1	350.9	473.9	1.53	19.68	20.41
EPDM-2	343.8	475.6	1.51	20.97	20.03
EPDM-3	339.8	476.1	1.50	22.79	19.67
EPDM-4	338.3	478.0	1.46	25.60	19.34
EPDM-5	337.7	481.1	1.43	28.72	19.03

stage of thermal decomposition at about 300 °C. Therefore, as the APP content increases, the thermal decomposition behavior of the composite material at 300 °C gradually increases, so the value of $T_{initial}$ gradually decreases. The delay in T_{max} is the result of the decomposition behavior of the second stage of APP, because the time when T_{max} is generated corresponds to the thermal decomposition process of EPDM molecular chains. During this process, the second stage of APP decomposition occurs and absorbs heat, reducing the heat transfer efficiency to EPDM. As a result, EPDM requires a higher temperature to reach its maximum decomposition rate, which in turn leads to an increase in T_{max}. As the APP content increases, the residual mass of the composite increases from 19.68 wt% to 28.72 wt%. Theoretical calculations of residual substances were performed. During the calculation process, the thermal decomposition behavior of APP and EPDM is referred to Fig. 3a and 4a. Aluminum hydroxide is completely converted into alumina, and the mass of silica remains unchanged. And the calculated results were compared with the actual test results. The results were compared with actual test results, as shown in Table 5. The theoretical results show that the final residual mass of the composite should slowly decrease as the APP content increases. However, actual results show that when the APP content is 15.9 wt%, the final residual mass of the composite material reaches 28.72 wt%, which is approximately 9.69 wt% higher than the theoretical calculation value. As seen from the curve in Fig. 4a, the addition of APP has no significant effect on the overall thermal decomposition step of EPDM composites. Therefore, it is speculated that APP does not affect the residue by directly acting on the carbonization of EPDM molecular chains. Instead, the formation of residual substances is promoted through the auxiliary effects of silica and aluminum hydroxide.

TG-IR technology can effectively detect the gaseous products released during the pyrolysis of materials. During the TG-IR test, nitrogen atmosphere was used to simulate the oxygen-poor environment in SRM and the thermal decomposition process of composite materials was studied in an oxygen-poor environment. The TG-IR results are shown in Fig. 5. A three-dimensional diagram of the TG-IR test results is presented in Fig. 5a. The total gas release as a function of time is illustrated in Fig. 5b. The gaseous products formed at 390 °C, 480 °C and 780 °C are shown in Fig. 5c. In the FT-IR spectrum, the characteristic peak of NH_3 gas appears at 390 °C, corresponding to the first-stage thermal decomposition behavior of APP. The peak at 480 °C corresponds to the gas phase decomposition products of the saturated hydrocarbons of EPDM rubber. As the temperature increases further, EPDM continues to slowly pyrolyze, accompanied by the second-stage thermal dehydration behavior of APP. The Gram–

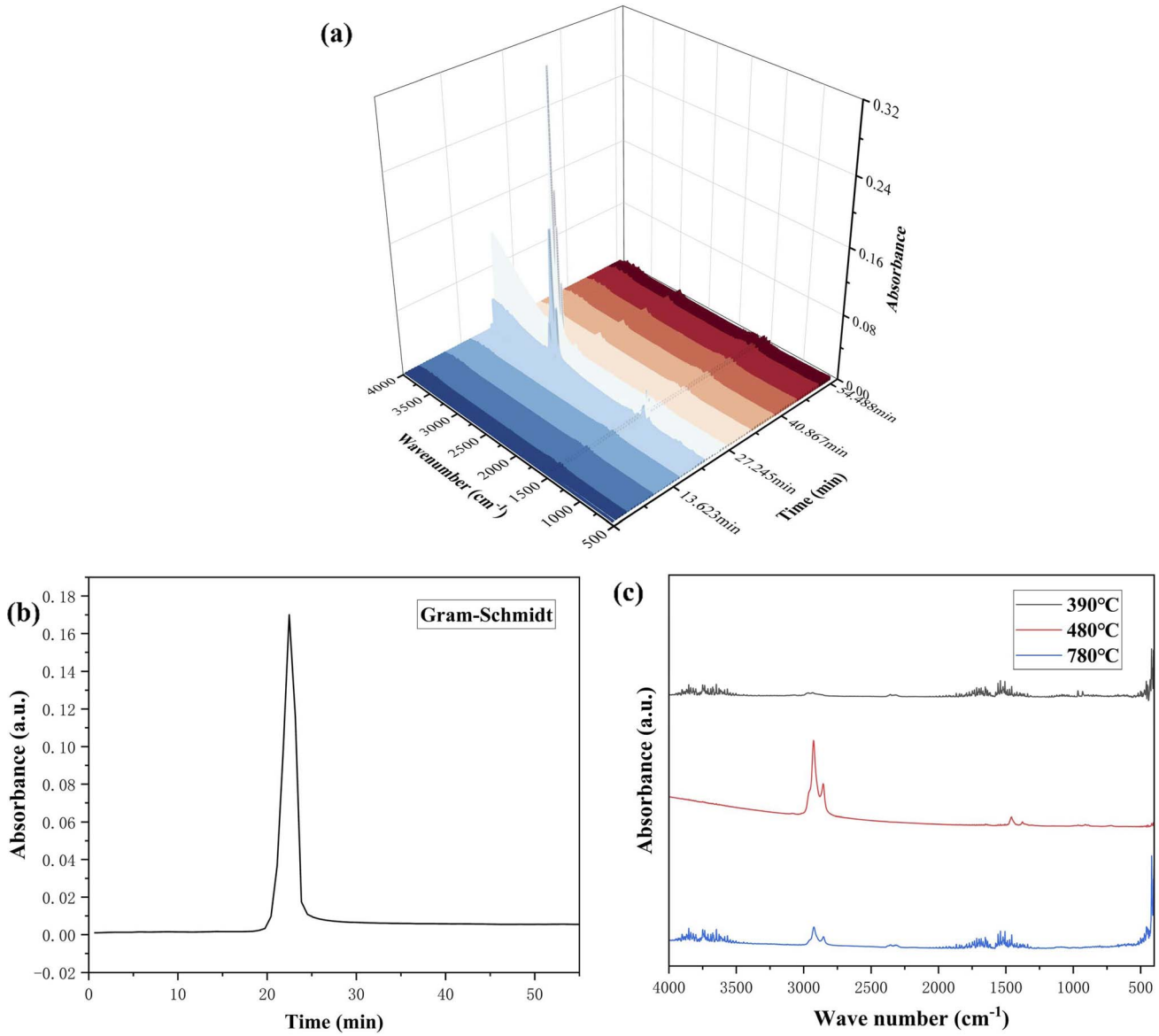

Fig. 5 (a) TG-IR analysis of EPDM-5 (b) Gram–Schmidt curve of EPDM-5; (c) infrared curve the gaseous product of EPDM-5 under different temperatures.

Schmidt curve shows that the gas product content in APP/EPDM composites decreases significantly after 500 °C. This may be due to the combined effect of the mixed gas composed of ammonia, water vapor and pyrolysis gas filled in the porous carbon layer formed by carbonization of EPDM and slowly released at high temperatures.[21–23] According to previous literature reports, NH_3 is converted into nitrogen gas and nitrogen oxides through free radical mechanism under the action of water vapor under oxygen-rich conditions.[24,25] These gases isolate oxygen and reduce the concentration of oxygen in the system to achieve the effect of improving flame retardant properties. However, in a nitrogen environment, no characteristic peak of NO is observed in the IR test results of the gas products produced by thermal decomposition of the composite material. This shows that NH_3 and water vapor generated by the thermal decomposition of APP are not further transformed. In fact, NH_3 and water vapor exert the flame retardant effect under oxygen-poor conditions.

3.4 Carbon layer analysis

Raman spectroscopy was used to study the degree of graphitization of carbon residue on the surface of the sample after testing. Under the action of the incident laser, the electrons in the valence band of single-layer graphene transition to the conduction band, and the electrons interact with phonons to cause scattering, which can produce different Raman characteristic peaks. Among them, the G peak is the main characteristic peak of graphite, which is caused by the in-plane vibration of sp^2 carbon atoms. It has E_{2g} symmetry and corresponds to the only first-order Raman scattering process in single-layer graphene. The D peak corresponds to a second-order double resonance Raman

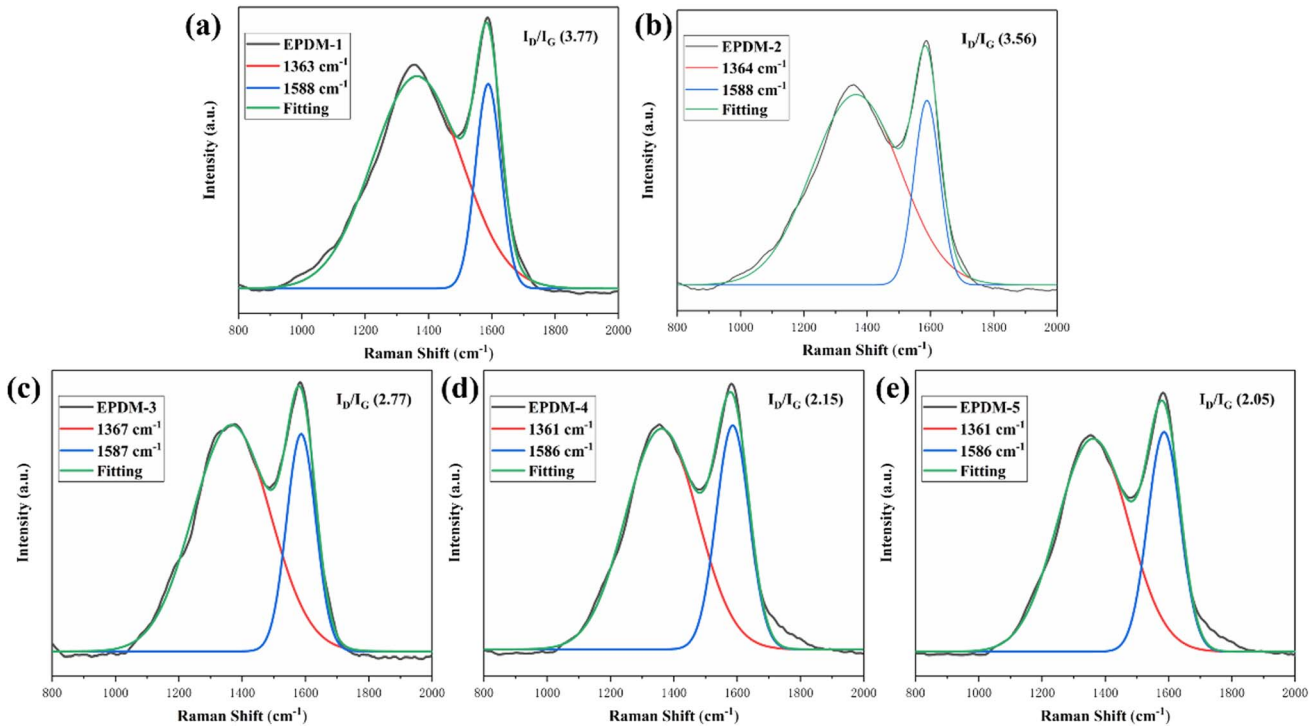

Fig. 6 Raman spectra of char for (a) EPDM-1, (b) EPDM-2, (c) EPDM-3, (d) EPDM-4 and (e) EPDM-5 after cone calorimeter tests.

process involving a defect scattering. The defects of graphene are reflected in its Raman D peak. Therefore, the degree of graphitization of the ablated sample can be calculated based on the integrated intensity ratio (I_D/I_G) between the D and G peaks. The lower the I_D/I_G, the higher the graphitization level of the sample. A high level of graphitization means that the carbon layer has high thermal stability and greater integrity, which can provide better protection.[26] Raman spectrum results show that as the APP content increases, the I_D/I_G of the carbon residue after ablation gradually decreases. This indicates that the degree of graphitization of carbon residue is significantly improved. The above result suggests that the improvement of the flame retardant behavior of the material by APP can make the surface carbon layer structure more complete, promote the densification of the

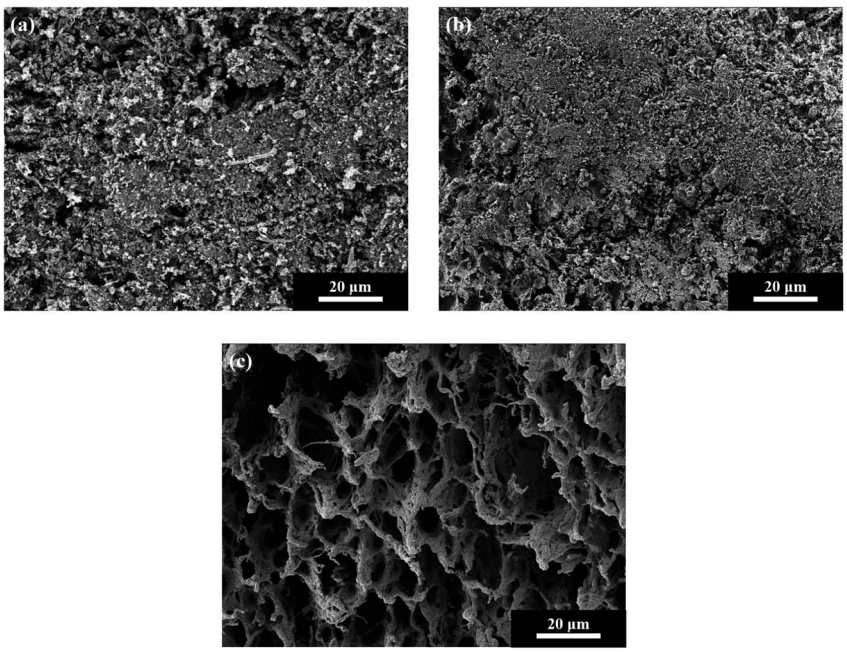

Fig. 7 SEM images of the surface layers of char residues of (a) EPDM-1, (b) EPDM-5 and the inner char layers of (c) EPDM-5.

surface carbon layer, and thereby improve the ablation resistance of the material (Fig. 6).

SEM images of the carbon layer of samples are shown in Fig. 7. The carbon layer of EPDM-1 presents obvious pores and cracks, as seen in Fig. 7a. This indicates that the carbon layer is less cross-linked and weaker. The large number of holes also suggests that a large amount of flammable gas escapes from the pores of the carbon layer of EPDM-1, and the material's flame retardant performance is low. In comparison, the carbon residue surface of EPDM-5 (Fig. 7b) has a denser morphology. This implies that the carbon layer can more effectively prevent gas from escaping from the holes and reduce the material exchange and energy exchange between the carbon layer and the gas phase.[27] As seen from Fig. 7c, the carbon layer of EPDM-5 has a loose and porous structure inside. This is conducive to the filling of the gas generated by the thermal decomposition of APP and the rubber matrix into the carbon layer, reducing the thermal conductivity inside the carbon layer. The SEM results show that after adding APP, EPDM-5 forms a carbon layer structure with a dense surface and a loose and porous interior. The dense carbon layer on the surface hinders the exchange of substances, while the loose and porous interior reduces the thermal conductivity inside the carbon layer through gas filling, limiting the exchange of energy. This decrease in exchange of matter and energy can improve the flame retardant properties of the material.

Elemental analysis of residues from TGA of APP/EPDM composites was performed by using EDS. The EDS results of the composite are shown in Fig. 8a and b. It is found that phosphorus element is evenly distributed on the surface of the carbon layer. This indicates that phosphorus-containing compounds formed by the thermal decomposition of APP are evenly distributed in the carbon layer. Elemental analysis was performed on the dense layer and porous layer of the carbon layer formed by EPDM-5, and the results are shown in Table 6. Compared with the porous layer, the contents of P and O elements in the dense carbon layer increase significantly, while the content of N element remains basically unchanged. In an oxygen-rich environment, EPDM undergoes thermal oxidation reactions at high temperatures, and carboxyl and hydroxyl groups are formed on the carbon skeleton.[28] Substances such as metaphosphoric acid and polyphosphoric acid generated by thermal decomposition of APP can undergo dehydration and carbonization reactions with the hydroxyl groups on the carbon layer skeleton formed by the decomposition of EPDM to form a carbon layer.[29,30] During this process, phosphorus is enriched in the carbon layer. However, in an oxygen-poor environment, the main chain with groups such as hydroxyl groups cannot be formed due to the thermal decomposition process of EPDM. Combined with EDS analysis results, it can be inferred that the phosphorus-containing substances formed by the thermal decomposition of APP move to the surface of the carbon layer driven by the pyrolysis gas. Then, they are enriched on the surface of the carbon layer under the action of silica and alumina fillers, preventing the pyrolysis gas from escaping. The vapor deposition reaction of small molecules formed by EPDM pyrolysis on the carbon skeleton is enhanced,[31] thereby increasing the density of the surface carbon layer.

Table 6 Elemental composition of EPDM-5 ablated sample

	Composition (%)				
EPDM-5	C	O	N	P	S
Dense layer	80.32	12.11	2.00	4.86	0.72
Porous layer	92.87	2.62	1.88	2.08	0.55

3.5 Flame retardant performance analysis

On this basis, the possible mechanism by which APP fillers improve the flame retardant properties of EPDM composites in oxygen-poor environments was explored. As shown in Fig. 9, APP can improve the flame retardant properties of EPDM flame retardant materials mainly through the following aspects. During the thermal decomposition process of the composite material, APP undergoes endothermic decomposition to generate non-flammable gases such as NH_3 and H_2O. At the

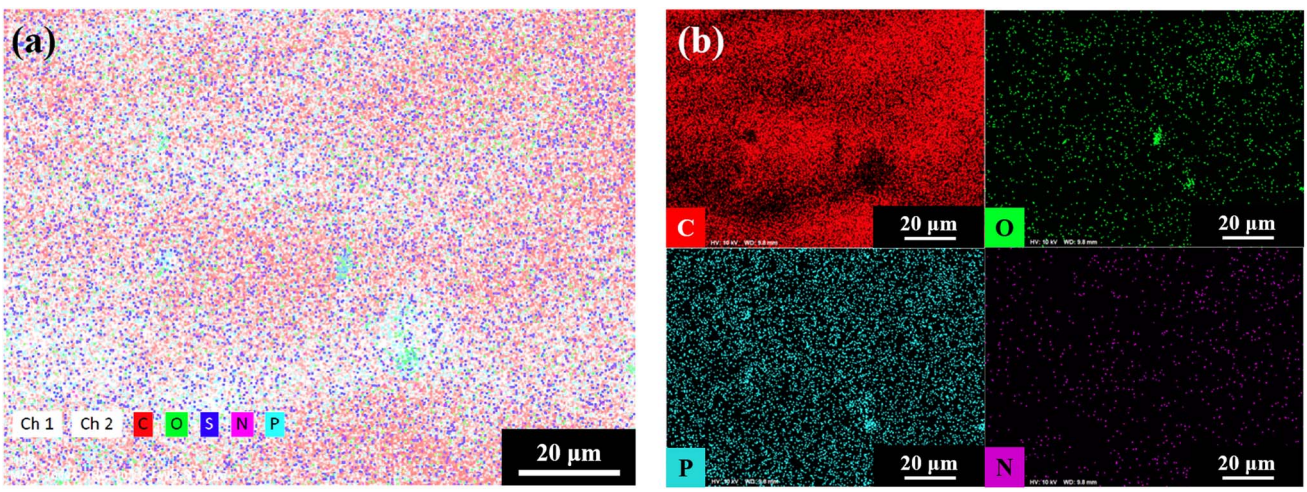

Fig. 8 EDS mapping results of char residues for EPDM-5.

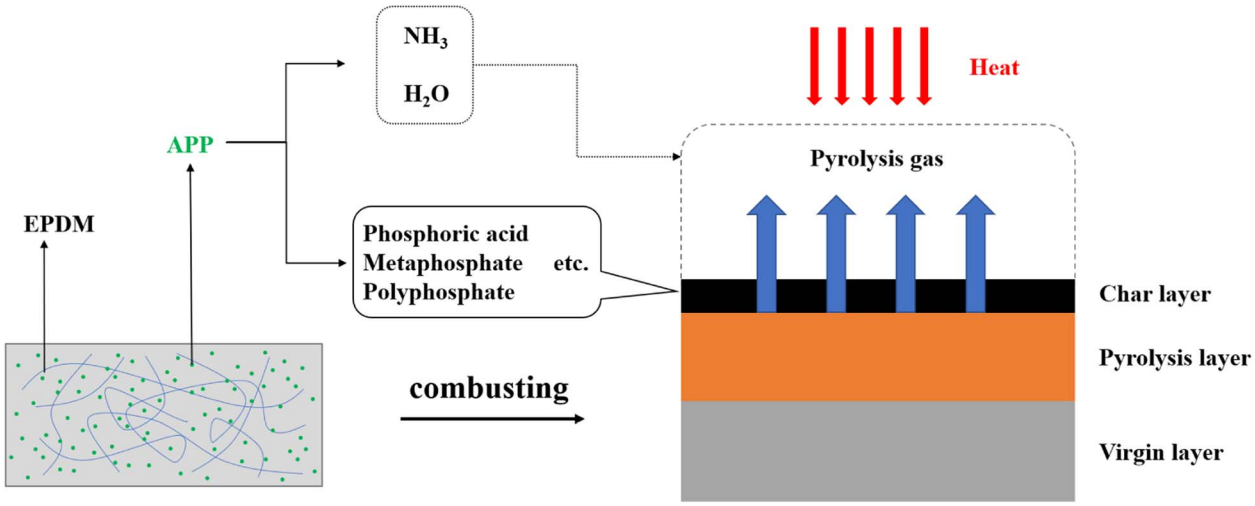

Fig. 9 Flame retardant mechanism of APP in EPDM.

same time, substances such as phosphoric acid, metaphosphoric acid, and polyphosphoric acid are generated. This is different from the flame retardant behavior of NH_3 in an oxygen-rich environment, which can consume oxidants through a series of free radical reactions such as capturing oxygen free radicals and hydroxyl free radicals. The flame retardant behavior of APP in the gas phase in an oxygen-depleted environment relies more on the low thermal conductivity and high thermal stability of the decomposed gas. On the one hand, the generation of NH_3 and H_2O gases can dilute the small molecular substances formed by the decomposition of the rubber matrix. On the other hand, the generated gas fills the holes in the carbon layer formed by the thermal decomposition of EPDM, reducing the thermal conductivity of the carbon layer. In the condensed phase, the decomposition of the rubber matrix in an oxygen-poor environment cannot provide hydroxyl groups on the carbon skeleton. APP decomposition products such as metaphosphoric acid and polyphosphoric acid cannot combine with them to undergo dehydration and carbonization reactions.[28,29] Therefore, these substances migrate to the surface of the rubber material under the influence of pyrolysis gas. Together with the fumed silica in the material and the alumina formed by thermal decomposition, they gather on the surface of the carbonized layer, hindering the material exchange and energy exchange between the gas phase and the pyrolysis layer. Under the protection of this carbon layer containing phosphorus–silicon compounds, the small molecular gases generated by EPDM pyrolysis are more likely to undergo chemical vapor deposition reactions at high temperatures, densifying the surface of the carbon layer. Thus, the flame retardant properties of the composite material are enhanced.

4 Conclusion

In summary, the flame retardancy of APP/EPDM composites with varying APP contents was evaluated using relevant characterization, performance and simulated burning tests. The results showed that the addition of APP did not significantly reduce the mechanical properties of the composite materials. TGA results showed that the APP/EPDM composite produced higher residues than the corresponding EPDM-1 sample. Compared with EPDM-1, the LOI of EPDM-5 composite containing 15.9 wt% of APP increased from 16.0 to 28.1. EPDM-5 passed the UL-94 vertical combustion test and reached V-0 level. The products formed by the thermal decomposition of APP in EPDM composite materials promoted the formation and density of the surface carbon layer in the condensed phase, significantly enhancing the flame retardant properties of the composite material. Understanding the thermal decomposition behavior of composite materials in an oxygen-poor environment can provide practical guidance for the selection of appropriate flame retardant fillers and preparation of SRM insulation layer materials that meet actual needs.

Conflicts of interest

There are no conflicts to declare.

Acknowledgements

This test part of this work was supported by Core Research Facilities of College of Chemistry and Molecular Sciences and Wuhan University Test Center. This work was supported by Hubei Key Laboratory of Advanced Aerospace Propulsion Technology Scientific research fund.

References

1 X. Jia, Z. Zeng, G. Li, D. Hui, X. Yang and S. Wang, Enhancement of ablative and interfacial bonding properties of EPDM composites by incorporating epoxy phenolic resin, *Compos. B Eng.*, 2013, **51**, 234–240.
2 J. Chen, W. Huang, S. B. Jiang, X. Y. Li, Y. An, C. Li, X. L. Gao and H. B. Chen, Flame-retardant EPDM compounds containing phenanthrene to enhance radiation resistance, *Radiat. Phys. Chem.*, 2017, **130**, 400–405.

3 H. Ismail, P. Pasbakhsh, M. N. A. Fauzi and A. Abu Bakar, Morphological, Thermal and tensile properties of halloysite nanotubes filled ethylene propylene diene monomer (EPDM) nanocomposites, *Polym. Test.*, 2008, **27**(7), 841–850.

4 K. George, S. Mohanty, M. Biswal and S. K. Nayak, Thermal insulation behaviour of Ethylene propylene diene monomer rubber/kevlar fiber based hybrid composites containing Nanosilica for solid rocket motor insulation, *J. Appl. Polym. Sci.*, 2021, **138**(9), 49934.

5 A. Nihmath and M. T. Ramesan, Studies on the role of hydroxyapatite nanoparticles in imparting unique thermal, dielectric, flame retardancy and petroleum fuel resistance to novel chlorinated EPDM/chlorinated NBR blend, *Res. Chem. Intermed.*, 2020, **46**(11), 5049–5068.

6 A. Nihmath and M. T. Ramesan, Development of novel elastomeric blends derived from chlorinated nitrile rubber and chlorinated ethylene propylene diene rubber, *Polym. Test.*, 2020, **89**, 106728.

7 Z. Bao, C. Flanigan, L. Beyer and J. Tao, Processing optimization of latex-compounded montmorillonite/styrene-butadiene rubber-polybutadiene Rubber, *J. Appl. Polym. Sci.*, 2015, **132**(8), 41521.

8 B. Yoon, J. Y. Kim, U. Hong, M. K. Oh, M. Kim, S. B. Han, J.-D. Nam and J. Suhr, Dynamic viscoelasticity of silica-filled styrene-butadiene rubber/polybutadiene rubber (SBR/BR) elastomer composites, *Compos. B Eng.*, 2020, **187**, 107865.

9 B. Zirnstein, D. Schulze and B. Schartel, The impact of polyaniline in phosphorus flame retardant ethylene-propylene-diene-rubber (EPDM), *Thermochim. Acta*, 2019, **673**, 92–104.

10 M. A. Soto-Oviedo, O. A. Araujo, R. Faez, M. C. Rezende and M. A. De Paoli, Antistatic coating and electromagnetic shielding properties of a hybrid material based on polyaniline/organoclay nanocomposite and EPDM rubber, *Synth. Met.*, 2006, **156**(18–20), 1249–1255.

11 Y. Y. Yen, H. T. Wang and W. J. Guo, Synergistic effect of aluminum hydroxide and nanoclay on flame retardancy and mechanical properties of EPDM composites, *J. Appl. Polym. Sci.*, 2013, **130**(3), 2042–2048.

12 S. Yan, Research progress of PP/metal hydroxid flame retardant, *J. Mater. Chem.*, 2009, **37**(5), 15–16.

13 G. Li, M. Sun and F. Ma, Effects of surface modification of aluminum hydroxide on the properties of flame retardant silicone rubber, *Silicone Material*, 2015, **29**(6), 458–461.

14 P. Ren, J. Chen and Y. Song, Study on the preparation on ultra-fine magnesium hydroxide flame retardant in different hydrothermal treatment methods, *Chem. Ind. Eng. Prog.*, 2005, **24**(2), 186–189.

15 H. T. Nguyen, K. T. Q. Nguyen, T. C. Le and G. M. Zhang, Review on the use of artificial intelligence to predict fire performance of construction materials and their flame retardancy, *Molecules*, 2021, **26**(4), 1022.

16 S. N. K. Usri, Z. Jamain and M. Z. H. Makmud, A Review on Synthesis, Structural, Flame retardancy and dielectric properties of hexasubstituted cyclotriphosphazene, *Polymers*, 2021, **13**(17), 2916.

17 Y. Liu, Z. Tang and J. Zhu, Synergistic flame retardant effect of aluminum hydroxide and ammonium polyphosphate on epoxy resin, *J. Appl. Polym. Sci.*, 2022, **139**, e53168.

18 L. Wan, C. Deng and Z. Zhao, Flame retardant of natural rubber: strategy and recent progress, *Polymer*, 2020, **12**(2), 429.

19 Y. Sun, B. Yuan, X. Chen, K. Li, L. Wang, Y. Yun and A. Fan, Suppression of methane/air explosion by kaolinite-based multi-component inhibitor, *Powder Technol.*, 2019, **343**, 279–286.

20 J. S. Wang, L. Xue, B. Zhao, G. D. Lin, X. Jin, D. Liu, H. B. Zhu, J. J. Yang and K. Shang, Flame retardancy, fire behavior, and flame retardant mechanism of intumescent flame retardant EPDM containing ammonium polyphosphate/pentaerythrotol and expandable graphite, *Materials*, 2019, **12**(24), 4035.

21 Z. H. Chang, F. Guo, J. F. Chen, L. Zuo, J. H. Yu and G. Q. Wang, Synergic flame retardancy mechanism of montmorillonite in the nano-sized hydroxyl aluminum oxalate/LDPE/EPDM system, *Polymers*, 2007, **48**(10), 2892–2900.

22 B. Yuan, Y. Sun, X. Chen, Y. Shi, H. Dai and S. He, Poorly-/well-dispersed graphene: Abnormal influence on flammability and fire behavior of intumescent flame retardant, *Composites, Part A*, 2018, **109**, 345–354.

23 Y. Sun, B. Yuan, S. Shang, H. Zhang, Y. Shi, B. Yu, C. Qi, H. Dong, X. Chen and X. Yang, Surface modification of ammonium polyphosphate by supramolecular assembly for enhancing fire safety properties of polypropylene, *Compos. B Eng.*, 2020, **181**, 107588.

24 Z. Zhao, T. Zhang, X. Li, *et al.*, NO formation mechanism of CH_4/NH_3 jet flames in hot co-flow under MILD-oxy condition: Effects of co-flow CO_2 and H_2O, *Fuel*, 2022, **313**, 123030.

25 C. Zhou, Y. He and Y. Song, The characteristics and mechanism of the NO formation during oxy-steam combusion, *Fuel*, 2015, **158**, 874–883.

26 W. M. Lu and Z. F. Jin, Synthesis of phosphorus/nitrogen containing intumescent flame retardants from p-hydroxybenzaldehyde, vanillin and syringaldehyde for rigid polyurethane foams, *Polym. Degrad. Stab.*, 2022, **195**, 109768.

27 K. Li, Y. Zou, S. Bourbigot, J. Ji and X. Chen, Pressure effects on morphology of isotropic char layer, shrinkage, cracking and reduced heat transfer of wooden material, *Proc. Combust. Inst.*, 2021, **38**(3), 5063–5071.

28 Q. Hu, Q. Chen and P. Song, Performance of thermal-oxidative aging on the structure and properties of ethylene propylene diene monomer (EPDM) vulcanizates, *Polymer*, 2023, **15**(10), 2329.

29 R. A. Vaia, G. Price, P. N. Ruth, H. T. Nguyen and J. Lichtenhan, Polymer/layered silicate nanocomposites as high performance ablative materials, *Appl. Clay Sci.*, 1999, **15**(1–2), 67–92.

30 W. Tang, Z. Sheng, X. Gu, J. Sun, X. Jin and H. Li, Effects of kaolinite nanoroll on the flammability of polypropylene nanocomposites, *Appl. Clay Sci.*, 2016, **132–133**, 579–588.

31 J. Li, K. Xi and X. Lv, Characteristics and formation mechanism of compact/porous structures in char layers of EPDM insulation materials, *Carbon*, 2018, **127**, 498–509.